Application of a Molecular Simulation Technique for Prediction of Phase-Separated Structures of Semirigid Model Polyurethanes

Hun-Jan Tao, Cun F. Fan,† William J. MacKnight, and Shaw L. Hsu*

Polymer Science and Engineering Department and Materials Research Laboratory, University of Massachusetts, Amherst, Massachusetts 01003

Received July 26, 1993; Revised Manuscript Received December 28, 1993●

ABSTRACT: A combination of a molecular simulation method and the Monte Carlo method has been successfully utilized to calculate phase diagrams of model polyurethanes. In our model, the entropic contribution of the Flory–Huggins expression has been modified to incorporate the contribution arising from orientation of hard segments. The constraint associated with chain rigidity of hard segments has been explicitly considered. In addition, the interaction term has been modified to include the relative packing of hard segments. Phase diagrams of various MDI–PPG model polyurethanes have thus been predicted utilizing these modifications. The effects of soft- and hard-segment lengths have been considered and the actual degree of phase separation calculated. Our predictions have been compared to experimental values. Additionally, the contribution of hydrogen bonding to the miscibility behavior of hard and soft segments needs to be reevaluated.

Introduction

The phase-separated structure associated with segmented polyurethanes is directly responsible for the properties observed for this class of thermoplastic elastomers.[1–3] These phase-separated structures can be complex, depending on the relative amount and type of hard/soft segments as well as their molecular weight, distribution, and temperature. The resultant structures have undergone extensive characterization.[1–3] Due to the increased availability of well-characterized hard and soft segments, the kinetics of morphology formation have also been characterized.[4,5] Despite extensive experimental studies, significant questions remain concerning fundamental aspects of phase separation behavior.[6–11] The formation of microphase-separated structures for segmented polyurethanes is generally accepted to arise from hard- and soft-segmented chemical incompatibility. However, in some instances, experimental data appear to be contradictory to this straightforward explanation.[6–9] Interactions between hard–hard segments should presumably be stronger than hard–soft interactions in order to phase separate and produce hard-segment-rich domains. Recently obtained spectroscopic data, however, suggest that the interactions, primarily formation of hydrogen bonds, between hard–soft segments are more favorable or stronger than interactions between individual hard–hard components.[8,9] Additionally, it has been shown that phase separation can still occur for non-hydrogen-bonded polyurethane systems.[3,12,13] Finally, crystallization of the hard segments is not necessarily the driving force and a requisite condition for phase separation. Numerous studies show that the structure in the hard-segment domains is not crystalline.[1,14–16]

Clearly, further analysis is necessary to support and guide experimental studies for improved understanding of the phase-separated structures of polyurethanes. A number of theories for prediction of polymer miscibility behavior have been presented.[17–19] Although, in some instances, the shape effect has been considered and specific interactions incorporated, a common assumption is that all chains are flexible. This assumption is inapplicable for consideration of miscibility behavior of hard–soft polyurethane segments. Greater emphasis has recently been focused on the effects of chain rigidity on miscibility behavior.[20–23] Hølyst and Schick, for example, proposed a rod–coil theory to calculate phase equilibrium behavior of rod–rod and rod–coil mixtures and rod–coil block copolymers.[22]

An alternate approach has been pursued in our laboratory. In a previous study, a combination of the Flory–Huggins theory and a molecular simulation technique was applied to miscibility studies of three types of binary mixtures including solvent with solvent, polymer with solvent, and polymer with polymer.[24] Molecular simulation is utilized to calculate the interaction parameter in the Flory–Huggins theory, including heat of mixing associated with pairwise interactions and the number of possible interaction partners, i.e., coordination number. The pair energies are obtained by averaging a large number of configurations generated by the *Monte Carlo* method as well as considering the constraint associated with excluded volume. The temperature dependence of the interaction parameter χ is obtained with the formalism developed in the earlier study. In several examples, the calculated upper critical solution temperatures were compared with experimental values. This combination of Flory–Huggins theory and the molecular simulation technique provides an opportunity to study the thermodynamic behavior of a binary mixture without possessing previous knowledge or experimental data for the systems considered.

To extend the applicability of the molecular simulation approach to polyurethane systems, the inherent chain rigidity needs to be considered, a concept encountered in studies of the isotropic–anisotropic transition of liquid crystalline polymers.[25] Flory, in deriving an isotropic to anisotropic transition in liquid crystalline polymers, considered the repulsive force associated with the chain rigidity effect. In such an instance, an anisotropic phase can coexist with an isotropic phase even if the interaction between polymer and solvent is favorable. Phase separation results from the entropic rather than enthalpic term. A positive χ parameter can enhance phase separation; Even a negative χ system may have phase separation, however. Chemical incompatibility is not requisite for phase separation if the difference in chain rigidity is significant.

A molecular simulation study with the following features has been conducted: (1) Prediction must be applicable

* To whom correspondence should be addressed.
† Permanent address: Molecular Simulations, Inc., Burlington, MA.
● Abstract published in *Advance ACS Abstracts,* February 15, 1994.

0024-9297/94/2227-1720$04.50/0

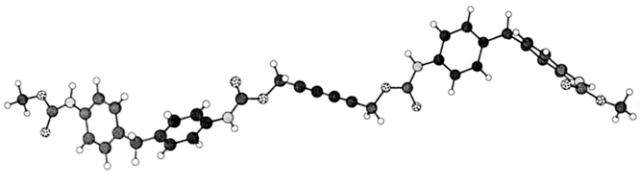

Figure 1. Schematic drawing of the single-chain structure of an M24M hard segment.

for a mixture of rod and flexible segments. (2) The existence of molecular parameters is identifiable with the polymers being studied. (3) Phase separation can occur even with a negative χ parameter. Furthermore, the relative importance of various secondary interactions is also of interest. An extension of our molecular simulation technique incorporating chain rigidity to explain polymer miscibility behavior is presented here.

Method

1. Chemical Structural Units Considered. The hard segments utilized in our simulation study are as follows: "M24M" designates one 2,4-hexadiyn-1,6-diol in the middle as the chain extender with an MDI [4,4′-methylenebis(phenyl isocyanate)] unit at each end. MDI units are capped with methyl groups. The structure is presented in Figure 1. Similarly, "M24M24M" refers to a hard segment with two 2,4-hexadiyn-1,6-diol units and three MDI units. The soft segments are PPG [poly(propylene glycol)] with molecular weights of 1000, 2000, and 3000. The hard segments are monodisperse in molecular weight. Schematic drawings of the monomer units are as follows:

MDI	$OCNC_6H_4CH_2C_6H_4NCO$
2,4-hexadiyn-1,6-diol	$HOCH_2C{\equiv}CC{\equiv}CCH_2OH$
PPG	$OH[CH_2C(CH_3)HO]_nH$

PPG is chosen as the soft segment in our experimental program to avoid complexities arising from soft-segment crystallization. Hard segments were chosen for numerous reasons: (1) Hard segments with short MDI units do not form crystalline hard-segment domains, and thus perturbing effects arising from crystallinity are eliminated. (2) The diacetylene segment is more rigid than the butanediol (BD) chain extender typically used, thus simplifying our calculation. (3) By studying photoreactivities and thermal reactivities of the diacetylene segment, some of our assumptions and calculations can be verified.[15]

2. Calculation of the Free Energy of Mixing. Extension of Our Previous Model. The actual calculation of the free energy of mixing, ΔG, depends on the specific theory or model employed, with the Flory–Huggins lattice method perhaps being the simplest. In the previous study, the basis for providing a methodology incorporating molecular simulation techniques for studies of mixing behavior of binary systems was developed.[24] The model is incomplete, as noncombinatorial entropic terms were not considered. In addition, interactions between polymers were approximated only by interactions between polymer segments occupying a similar *lattice* size. A question arises as to how accurate pairwise interactions, Δw_{ij}, can be obtained to represent interactions in the actual condensed phase. Use of molecular mechanics to minimize energy using several selected configurations was determined not to be representative of the interaction energy for binary mixtures exhibiting normal Boltzmann distributions. Since relative movement of the two interacting segments is quite small at low temperatures, molecular dynamics samples only localized configurational space, unless very fast computers are utilized; therefore, they cannot provide accurate interaction terms easily. From the pragmatic view, to improve the reliability of calculation of Δw_{ij} as a function of temperature, including constraints arising from excluded volume, an approach incorporating the *Monte Carlo* technique was established to take into account and properly weigh a large number of relative orientations of the two molecules. In order to eliminate bias introduced by the chosen configurations, a crucial step for reliable calculation of interaction energies, ΔW's, is to establish an efficient algorithm for sampling relative orientations of a pair of interacting molecules. By calculating the specific interaction energies of the configurations which satisfied Metropolis statistics, we were able to calculate the interaction energy at various temperatures.[24]

Table 1. Structure, Volume, and the Average Size of the Subunits Calculated for the Hard and Soft Segments

	structure	volume (Å^3)	average size (Å)
hard segment			
subunit-1	$O(C{=}O)NH$	143.27	5.2
subunit-2	$CH_2C{\equiv}C$	131.08	5.1
subunit-3	C_6H_4	196.5	5.8
soft segment			
subunit	$CH_2C(CH_3)HO$	284.77	6.6

In this study, to satisfy a requirement for use of the lattice model in calculating the interaction energy between hard and soft segments, each hard segment is divided into several subunits occupying a volume similar to the PPG soft segment. The M24M hard segment is then decomposed into four subunit-1, two subunit-2, and four subunit-3. M24M24M consists of six subunit-1, four subunit-2, and six subunit-3. The structures of the subunits are given in Table 1 where their volumes are defined as the volumes within the van der Waals surfaces and calculated by the uniform finite element method.[26] The cubic root of the volume is taken as the average size for each subunit. Traditionally, the interaction energy, ΔW_{hs}, for the two types of entities with similar size and spherical symmetric geometry can be defined as

$$\Delta W_{hs} = W_{hs} - \frac{1}{2}(W_{hh} + W_{ss}) \tag{1}$$

where W_{ij} is the intermolecular interaction between i and j. "h" denotes the hard segment, and "s" denotes the soft segment. The interaction parameter, χ, is defined as

$$\chi = Z\Delta W_{hs}/RT \tag{2}$$

where Z is the coordination number. The uncertainty in this number will influence the critical temperatures calculated, in some cases, significantly. This number can be determined by methods described earlier.[24] The most simplistic way is to calculate the cohesive energy density of one or more pairs of interacting segments using periodic boundary conditions. Our earlier studies have shown that various techniques yield a value of 6–7 for the systems described. In addition, with $Z = 6$, the calculated critical temperatures fit experimental data most accurately for the molecular or polymeric systems studied.[24] Therefore, in this study, we have used the number 6 for every segment pair as an assumption. Pairwise secondary interactions including van der Waals and hydrogen bonding are explicitly considered. By assuming that the interaction energy is proportional to the numbers of subunits in the hard segment, the hard–soft segment interaction, W_{hs}, for the M24M/PPG system is calculated as

$$W_{hs} = \frac{1}{10}(4E_{s1} + 2E_{s2} + 4E_{s3}) \tag{3}$$

where E_{si} represents the intermolecular interaction between the soft segment and subunit i in the hard segment. Similarly for the hard–hard segment interaction, W_{hh}, we have

$$W_{hh} = \frac{1}{100}(16E_{11} + 16E_{12} + 32E_{13} + 4E_{22} + 16E_{23} + 16E_{33}) \tag{4}$$

In a similar fashion, the interaction energies of the M24M24M/PPG system are

$$W_{hs} = \frac{1}{16}(6E_{s1} + 4E_{s2} + 6E_{s3}) \tag{5}$$

$$W_{hh} = \frac{1}{256}(36E_{11} + 48E_{12} + 72E_{13} + 16E_{22} + 48E_{23} + 36E_{33}) \tag{6}$$

In these cases, we have assumed that the probability of contact points is identical along the chain. The E_{ij}'s represent interactions between i and j subunits of the hard segment. This assumption

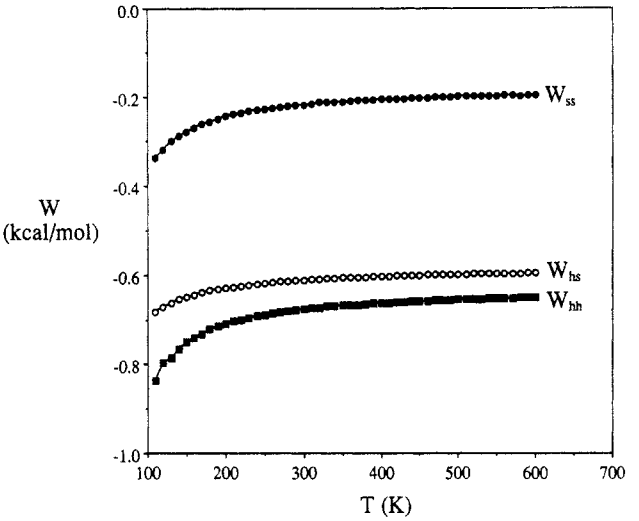

Figure 2. Calculated interaction energy terms between hard and soft segments for the M24M/PPG model system.

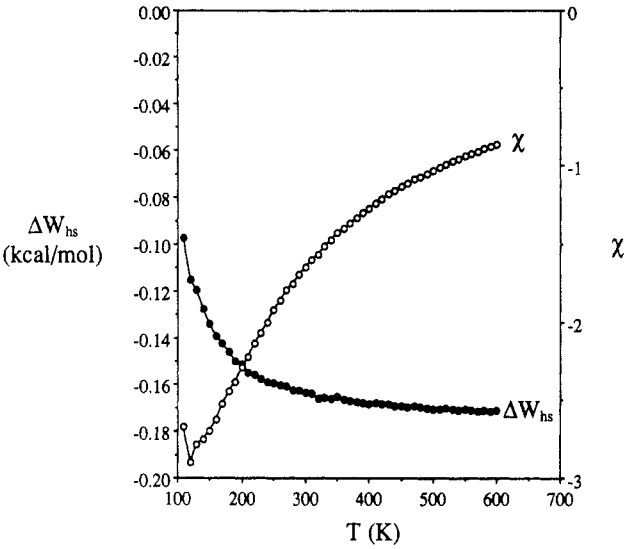

Figure 3. Simulated interaction energy ΔW_{hs} and the χ parameter for the M24M/PPG model system.

is adequate for flexible hard segments in either hard-segment-rich or soft-segment-rich domains. For the case of rigid hard segments, this approximation assuming that contact points between two rods are random remains adequate for the isotropic phase as there is no preferential orientation between the two chain segments. In other words, the defined enthalpic interactions are consistent with the Flory–Huggins model. It is obvious that this is not the case for rigid hard segments in the hard-segment-rich domains because, in this case, the hard segments display preferential orientation between themselves. It is therefore necessary to introduce another parameter, V, as described below, to describe the enthalpic contribution to the free energy.

The classical force-field characteristic of interatomic interactions, whether intramolecular or intermolecular, is the single most important and essential parameter governing the accuracy of simulation techniques. The energy of a system, which can be a single molecule, a pair of molecules, or even a condensed state assembled with a large number of molecules, is defined by different energy terms. Covalent interactions may be described by terms such as bond, valence angle, torsion, and hybridization. Terminology describing nonbonded interactions includes van der Waals, electrostatic, and hydrogen-bonding interactions. The specific force field used in our study has been previously defined.[27] The *POLYGRAF* software is from Molecular Simulations, Inc. The necessity for incorporating partial charges depends on the specific force fields used. Some contributions from charges have been incorporated in the force field.[27] It has been shown that explicit incorporation of charges appears unnecessary.

The interaction energies for various pairwise interactions of the M24M/PPG system calculated as a function of temperature are shown in Figure 2. The M24M24M/PPG system shows a similar result. In both cases, the hard–hard segmental interaction, W_{hh}, is the most favorable and the soft–soft interaction, W_{ss}, the least favorable. The calculated interaction energy, ΔW_{hs}, and the χ parameters, both negative, are shown in Figure 3. The negative χ values obtained suggest that phase separation should not occur in the temperature range of interest according to the Flory–Huggins theory, in direct contradiction to known polyurethane morphology. This inherent contradiction arises from either the simulation technique, including force field, or inapplicability of the Flory–Huggins theory to polyurethane elastomers. Accurate structural predictions for a broad spectrum of molecules and macromolecules have demonstrated the reliability of the force field.[24,27] The simulation technique, including the *Monte Carlo* method proposed, has also proven effective.[24] Experimental data have shown that a negative χ is possible for the polyurethanes, and our calculated χ values are in reasonable agreement with those measured.[6,7] For example, χ parameters can be as low as −3 for systems with relatively weak specific interactions and as low as −12 for those with strong specific interactions.[28]

3. Modifications of Earlier Algorithms. The principal deficiency with use of the Flory–Huggins theory is that it is applicable only for flexible chains. Modification of the theory incorporating chain rigidity is thus necessary for polyurethanes. The model hard segment of M24M in the single chain conformation is shown in Figure 1. In the MDI unit, the rotational barrier of various dihedral angles can be in the range of 1.8–7 kcal/mol. There is little possibility for chain conformation to deviate from the straight segment shown schematically in Figure 1, thus making it impossible to satisfy the basic assumption of the Flory–Huggins theory, i.e., flexible chains. The theory for prediction of mixing behavior needs to be modified to include the following:

1. Accommodate a mixture of rigid and flexible chains.
2. Include parameters which can be predicted by the molecular simulation method.
3. Predict phase separation even with negative interaction parameters.

Consideration of the original formalism of Flory's liquid crystal theory to the isotropic–anisotropic transition appears relevant.[29] In that theory, upon increasing the rod concentration beyond a critical value, the system phase separates into one isotropic and one anisotropic phase even if favorable interactions exist between the rod and solvent. The driving force arises from not only the enthalpic but also entropic term associated with relative chain orientation. When the solvent is replaced by the random coil, and if the coil length is sufficiently long, the connectivity between the hard and soft segments can be ignored and thermodynamic equations simplified to a rod–coil blend system.[30,31] It has also been shown that an anisotropic phase of pure rods can be formed if the coil length is sufficiently long.

Extending Flory's rod–coil theory, the chemical potentials for the hard segment unit, 2, and the soft segment unit, 3, in the isotropic phase (soft-segment-rich domains) and the ordered phase (hard-segment-rich domains) have been derived as shown below. In these expressions, it is assumed that the same χ exists in the isotropic and anisotropic/ordered phases.

Anisotropic/Ordered Phase

$$\frac{\mu_2' - \mu_2^0}{RT} = \ln\left(\frac{\phi_2'}{N_2}\right) + \phi_2'(y-1) + \phi_3' N_2\left(1 - \frac{1}{N_3}\right) + 2(1 - \ln y) + \chi N_2 \phi_3'^2 \quad (7)$$

$$\frac{\mu_3' - \mu_3^0}{RT} = \ln\left(\frac{\phi_3'}{N_3}\right) + \phi_2'\left(\frac{N_3}{N_2}\right)(y-1) + \phi_3'(N_3 - 1) + 2\left(\frac{N_3}{y}\right) - \ln Z_3 + \chi N_3 \phi_2'^2 \quad (8)$$

Isotropic Phase

$$\frac{\mu_2 - \mu_2^0}{RT} = \ln\left(\frac{\phi_2}{N_2}\right) + \phi_2(N_2 - 1) + \phi_3 N_2\left(1 - \frac{1}{N_3}\right) - 2\ln N_2 + \chi N_2 \phi_3^2 \quad (9)$$

$$\frac{\mu_3 - \mu_3^0}{RT} = \ln\left(\frac{\phi_3}{N_3}\right) + \phi_2 N_3\left(1 - \frac{1}{N_2}\right) + \phi_3(N_3 - 1) - \ln Z_3 + \chi N_3 \phi_2^2 \quad (10)$$

where the disorder parameter, y, is determined by

$$\exp\left(-\frac{2}{y}\right) = 1 - \phi_2'\left(1 - \frac{y}{N_2}\right) \quad (11)$$

In the above expressions, N_2 is the axial ratio or number of rod subunits, N_3 is the degree of coil polymerization, ϕ is the volume fraction calculated in terms of the number of each subunit, Z_3 is the internal configuration partition function for the coil, μ is the chemical potential in the isotropic phase, and μ' is the chemical potential of the ordered phase. χ's can be calculated by using the molecular simulation method developed earlier. At equilibrium, the chemical potentials must be the same for each species in the two phases. It is then possible to derive the phase diagram using eqs 7–11.

The chemical potentials as a function of composition for the M24M/PPG-2000 system are shown in Figure 4. The phase diagrams can be determined only by setting eq 7 equal to 9, and eq 8 to eq 10, and seeking a simultaneous solution, subject to the condition imposed by eq 11. In our case, as found previously for rods mixed with long coils,[30,31] this is impossible. The only possible solution is for the ordered phase containing only hard segments to coexist with a phase of hard segments dispersed in the soft segments. Any phase composition falling within the heterogeneous phase region will separate into these two phases. The calculated phase diagram is shown in Figure 5. All the compositions falling within the isotropic phase region cannot exhibit phase separation and only a single phase can occur. While this calculation successfully demonstrates the phase separation tendency for our model polyurethane with a negative χ, the phase diagram indicates excessive phase mixing. For example, the calculation fails to predict phase separation for the M24M/PPG-2000 system (ϕ_2 = 0.227) at room temperatures when phase-separated structures are known to occur. This is due to the fact that the χ parameter used is inadequate to describe the enthalpic term for the ordered phase. As mentioned above, the χ parameter is calculated by assuming random orientation for the chain segments. For the rigid hard segments in the hard-segment-rich domain, this approximation is incorrect. An obvious solution is to use an enthalpic expression which takes into consideration the relative hard-segment orientation in this phase. In comparison to randomly oriented hard segments, the interactions between oriented segments are more specific and stronger and thus capable of shifting the phase boundary to lower values.

For a perfectly ordered state of hard segments, $y = 1$ and only varies in the isotropic phase, reaching a maximum value of N_2 for the completely disordered state. In Figure 4, the phase boundary is defined by the simultaneous solution of eqs 7–11. If the solution for y is less than 1 for the perfectly ordered state, then y is taken to be 1. This is seen as the peak in curve 4. The chemical potentials for soft segments exhibit a large difference at the isotropic and anisotropic boundary because the phase with soft segments dispersed in the isotropic state is favorable. Conversely, for soft segments to be confined in the ordered phase is rather unfavorable. For hard segments, on the other hand, the crossover from a very imperfect ordered state to the completely random isotropic phase is smoother.

4. Additional Considerations of Cohesive Energy of Hard Segments. An interaction parameter, V, is introduced to describe the strong cohesive energy in the hard-segment-rich domain which further stabilizes these domains to enhance phase separation. The enthalpic terms are derived from earlier studies on liquid crystalline polymers.[32-34] The modified expressions suitable for our system are shown below:

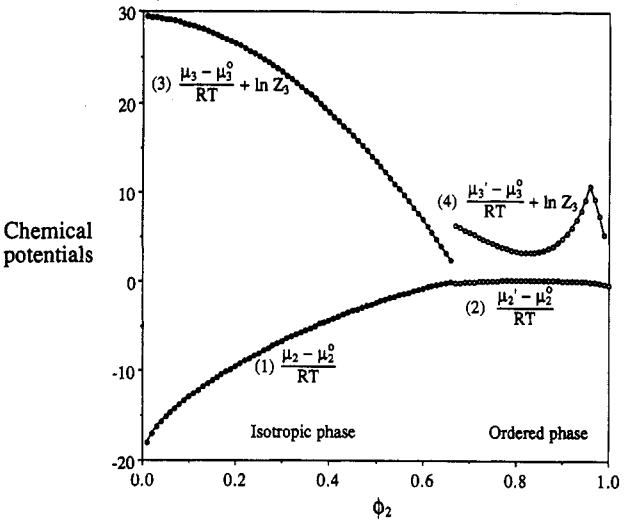

Figure 4. Simulated chemical potentials for the M24M/PPG model system by using Flory's rod–coil model: (1) Hard segments in the isotropic phase. (2) Hard segments in the anisotropic/ordered phase. (3) Soft segments in the isotropic phase. (4) Soft segments in the anisotropic phase.

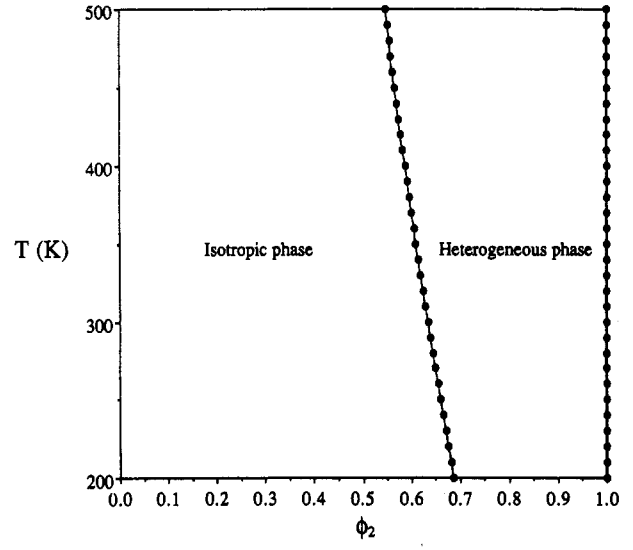

Figure 5. Simulated phase diagram for the M24M/PPG-2000 model system. ϕ_2 is the number fraction of the hard-segment subunits.

$$\frac{\mu_2' - \mu_2^0}{RT} = \ln\left(\frac{\phi_2'}{N_2}\right) + \phi_2'(y - 1) + \phi_3' N_2\left(1 - \frac{1}{N_3}\right) + 2(1 - \ln y) - \left(\frac{\phi_2'\langle P_2\rangle}{RT/V}\right)\left(1 - \frac{\phi_2'\langle P_2\rangle}{2}\right) \quad (12)$$

$$\frac{\mu_3' - \mu_3^0}{RT} = \ln\left(\frac{\phi_3'}{N_3}\right) + \phi_2'\left(\frac{N_3}{N_2}\right)(y - 1) + \phi_3'(N_3 - 1) + 2\left(\frac{N_3}{y}\right) - \ln Z_3 + \frac{\phi_2'^2\langle P_2\rangle}{2\left(\frac{RTN_2}{V}\right)} \quad (13)$$

with

$$P_2 = \frac{1}{2}(3\cos^2\theta - 1) \quad (14)$$

$$y = N_2\langle\sin\theta\rangle + 1 \quad (15)$$

$$\langle P_2\rangle = 0.99972 - 0.9596(RT/V) - 2.2413(RT/V)^2 \quad (16)$$

where V is the cohesive energy term between hard segments packed in a parallel manner, P_2 is the second-order Legendre

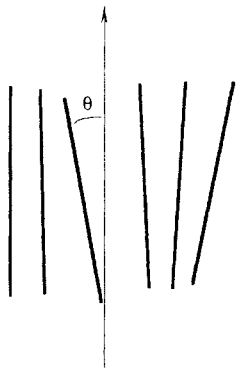

$$E(\cos\theta) = -V P_2(\cos\theta) \langle P_2 \rangle$$

Figure 6. Schematic drawing of the orientational order associated with hard segments. V is the Maier–Saupe interaction term between hard segments in the ordered phase. $E(\cos\theta)$ is the mean cohesive energy associated with imperfect hard-segment packing. $\langle P_2 \rangle$ is the order parameter.

polynomial, $\langle P_2 \rangle$ is the order parameter, and θ is the angle between the chain axis of one hard segment and the average orientational direction of the hard segments bundle (Figure 6).[34] In eqs 12 and 13, following Flory's approach, the enthalpic terms of the ordered domains are determined only by hard-hard segment interactions while the soft–soft and soft–hard segment interactions have been ignored. As described previously, coil penetration into hard-segment-rich domains is unlikely due to thermodynamic instability.

The interaction parameter, V, of two M24M segments has been approximated by using the average energy of two extremely different geometries. The first structure incorporates two molecules face-to-face, thus minimizing the hydrogen-bond contribution (8.40 kcal/mol), and a second geometry, with chains side-by-side with favorable hydrogen bonds (V = 21.46 kcal/mol). Based on our two calculations, V has been determined to be 15 kcal/mol for M24M, the average of the extreme values. The V value has no relation to the W_{hh}, which is the average pair interaction between two subunits of the hard segment assuming no preferential orientation between them and that their contact points are randomly determined. W_{hh} is used for calculation of the χ parameter in the isotropic phase while the V parameter is used for the ordered phase. The order parameter, $\langle P_2 \rangle$, in the ordered phase decreases with temperature. Equation 16 is a sufficiently accurate approximation for $RT/V < 0.1$,[34] which is typically the case. Phase diagrams of binary systems, including semirigid polymers, can be analyzed using such a formalism. We found that variation in the *coordination number*, Z, does not affect the phase diagrams calculated.

Results and Discussion

The recalculated chemical potentials of hard segments in the two different phases at different temperatures are shown in Figure 7. Several points need to be emphasized:

(1) For a sufficiently long coil and by solving eqs 9–16, the only possible solution suggests the existence of a phase containing pure hard segments. Coils are quite unlikely to penetrate into the ordered phase, decreasing the cohesive interactions between the hard segments and increasing their chemical potentials. The coil–rod interaction in the ordered phase and the existence of an interphase have been ignored.

(2) As the ordered phase consists only of hard segments, based on Figure 7, the composition in the isotropic phase, ϕ_2, can be determined by the condition

$$\mu_2(\phi_2) = \mu_2(\phi_2'=1) \tag{17}$$

Figure 8 shows the predicted phase diagram for M24M/PPG-2000 and M24M24M/PPG-2000 model systems. If the overall hard-segment concentration falls within the heterogeneous phase region, as in our case, it will phase separate into a pure hard-segment phase coexisting with a soft-segment-rich phase. The composition is shown by curves 1 and 2 in Figure 8. By considering the orientation effect of the hard segments in the hard-segment-rich domain with the interaction term, V, the prediction of phase-separation behavior in the same temperature range has been improved in comparison to the result for the M24M/PPG-2000 system shown in Figure 4.

(3) In this model, it is unnecessary for the ordered phase to form a crystalline structure to achieve phase separation. The driving force is the rigidity of the hard segment rather than crystallization. At best, most wide-angle X-ray diffraction patterns obtained for polyurethanes exhibit relatively broad peaks.[1,15,16] Although crystallization of hard segments is not necessary for phase separation, it can enhance it.

(4) If the hard and soft segments are chemically incompatible, i.e., with a positive χ, curves 1–3 in Figure 7 will shift upward, prohibiting phase mixing. Even for a negative χ, phase separation can occur if the Maier–

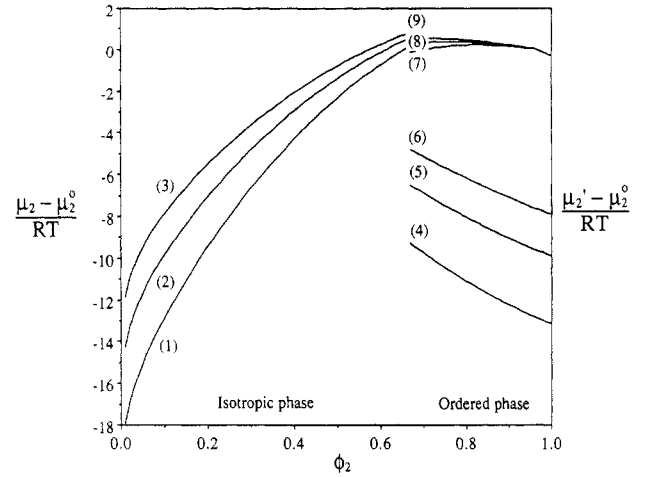

Figure 7. Simulated chemical potentials for the M24M/PPG-2000 system at different temperatures: for the isotropic phase at temperatures of (1) 300, (2) 400, and (3) 500 K; for the ordered phase at temperatures of (4) 300, (5) 400, and (6) 500 K (the V interaction term is 15 kcal/mol); for the ordered phase at various temperatures of (7) 300, (8) 400, and (9) 500 K, but without the Maier–Saupe modification.

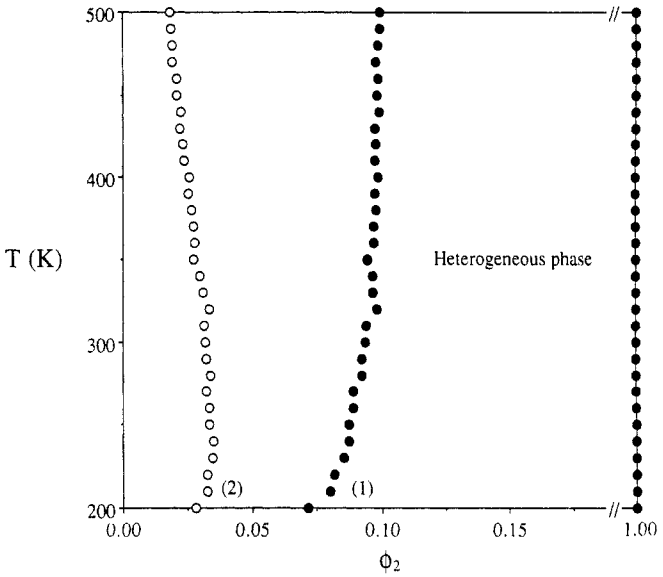

Figure 8. Effect of the hard-segment length on the phase diagram: (1) M24M/PPG-2000 model system with V equal to 15 kcal/mol. (2) M24M24M/PPG-2000 model system with V equal to 24 kcal/mol.

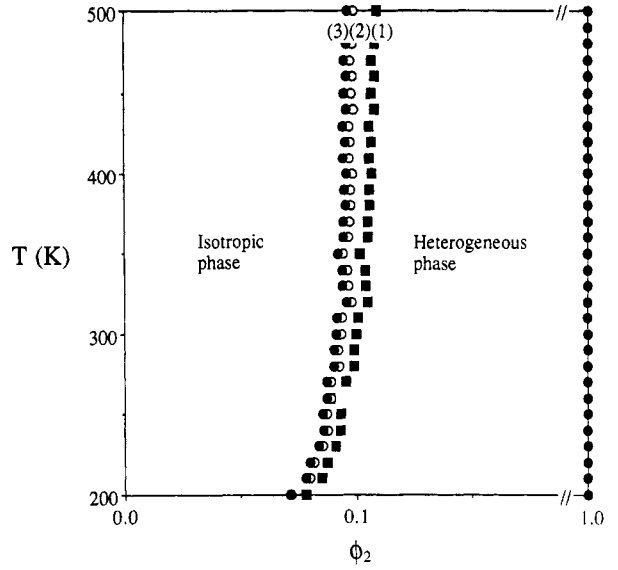

Figure 9. Effect of the soft-segment length on the phase diagram: (1) M24M/PPG-1000; (2) M24M/PPG-2000; (3) M24M/PPG-3000. The Maier–Saupe V parameter is taken to be 15 kcal/mol for all cases.

Saupe type interaction parameter, V, is sufficiently strong. Chemical incompatibility is not requisite for phase separation.

(5) Details of the phase equilibrium diagram are determined by the temperature variation of the χ term for the isotropic phase and the V term for the ordered phase.

Effects of Hard and Soft Segment Size. Phase diagrams for semirigid polyurethanes as a function of temperature and hard and soft segment molecular weights are presented in Figures 8 and 9. Polyurethane phase behavior has been studied using most of the common characterization techniques such as mechanical spectroscopy, thermal analysis, electron microscopy, and infrared spectroscopy.[1,2] Even though it is accepted that phase separation occurs, only a few studies have quantitatively demonstrated the degree of phase separation and the exact parameters which can influence the phase behavior.[13,14,35-38] Quantitative interpretation of experimental data depends on the morphological model used, e.g., whether to include an interphase.[36] Temperature is known to have but a weak effect on the phase composition. There is no evidence that the critical temperature lies within the 200–400 K temperature range.[38,39] Furthermore, the measured composition of the two individual phases is very dependent on the techniques used.

Very limited experimental studies have been directed at polyurethanes incorporating hard segments containing diacetylene chain extenders and only for polyurethanes containing short hard segments, usually 2 or 3 MDI units.[15,40] It is possible, however, to compare our calculations to similar systems containing more flexible hard-segment chain extenders, butanediol (BD), for example. Even then, quantitative analyses are quite rare. One analysis of the phase-separated structure, more specifically a relatively pure hard-segment-rich domain coexisting with a soft-segment-rich domain mixed with hard segments, as well as an interphase, is based on scattering and changes in the glass transition temperature.[36,38] Other calculations utilize the association model based on infrared results.[19,39] All of these studies show that the phase composition is virtually insensitive to temperature, at least in the range of interest. The generally accepted value of the degree of phase separation ranges from 30 to 90% for PPG–BD–MDI systems.[36,37] For polyurethanes containing 30% hard segments, a system close to ours, the composition in hard-segment-rich domains is estimated to be 57% of hard segments by X-ray and 84% by DSC.[36] The purity of the hard-segment-rich domain can never exceed 83% for longer hard segments by X-ray. NMR, however, shows that this domain can be virtually 100% hard segments for a model polyurethane with piperazine-based hard segment.[13] Thermal analysis data also indicate that with a change in the hard-segment length from 3 to 4 MDI units, the purity of the hard-segment-rich domains increases significantly from 57 to 78%.[36] The composition of the soft-segment-rich phase is estimated to be about 10–30% of hard segments by weight using X-ray and about 20–28% by DSC.[36] Since, as previously noted, the exact phase composition determined by various experimental techniques differs considerably, simulation techniques in fact can provide a better understanding of phase composition in phase-separated structures.

Our calculations are based on the model that hard-segment-rich domains are entirely pure hard segments. Our calculated results suggest that this phase coexists with another one containing both hard and soft segments. Generally speaking, our calculated results shown in Figures 8 and 9 show that longer hard segments or longer soft segments will cause lower hard-segment concentration in the soft phase, as expected. From Figure 9, it is also possible to conclude that the soft-segment length has only a minor effect on phase composition. Conversely, the hard-segment length can significantly perturb phase composition. For polyurethanes containing 2 MDI units, we preclude that soft-segment domains contain approximately 10% hard segments. This number decreases significantly to ~2.5% when the hard-segment length is increased to 3 MDI units (Figure 8). For polyurethanes containing 2 MDI units, changing the PPG soft-segment molecular weight from 1000–3000 does not significantly affect the phase diagram.

To quantitatively define the phase-separated structure, it is most convenient to use the parameter associated with the fraction of overall hard segments in the hard-segment-rich domains, F_{HH}, which can be calculated using values derived from Figures 8 and 9. F_{HH} can be calculated using the following expression only with the availability of the total number fraction of hard-segment subunits in the whole system, ϕ_{2T}, and the composition of the isotropic phase of the hard-segment subunit.

$$F_{HH} = \frac{\phi_{2T} - \left(\frac{1-\phi_{2T}}{1-\phi_2}\right)\phi_2}{\phi_{2T}} \qquad (18)$$

For our system, the ϕ_{2T}'s are 0.227 and 0.320 for M24M/PPG-2000 and M24M24M/PPG-2000, respectively. The calculated temperature dependence of the phase separation for different hard-segment lengths is summarized in Figure 10. Longer hard segments have higher F_{HH} values. Available DSC and X-ray experimental results at room temperature also show this trend.[36] The variation of F_{HH} values for different hard-segment lengths, however, is not as large as our calculation which is based on semirigid diacetylene chain extenders (~65% for 2 MDI units and 95% for 3 MDI units). Previous experimental data using DSC indicate that F_{HH}'s for the more flexible BD chain extenders range from 30% (3 MDI units) to 89% (14 MDI units).[36]

This difference between predicted and experimental values derived from DSC may arise from inherent limitations associated with the thermal analysis technique. The degree of phase separation estimated by DSC is based

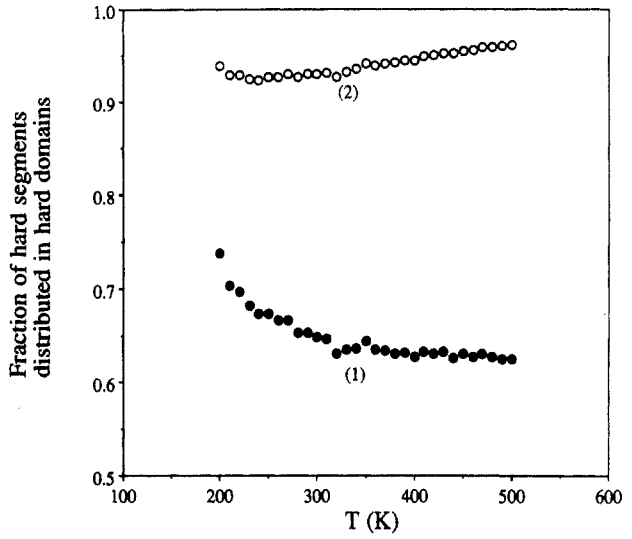

Figure 10. Effect of the hard-segment length on the fraction of hard segments distributed in the hard-segment-rich domain, F_{HH}: (1) M24M/PPG-2000 model system with V equal to 15 kcal/mol; (2) M24M24M/PPG-2000 with V equal to 24 kcal/mol.

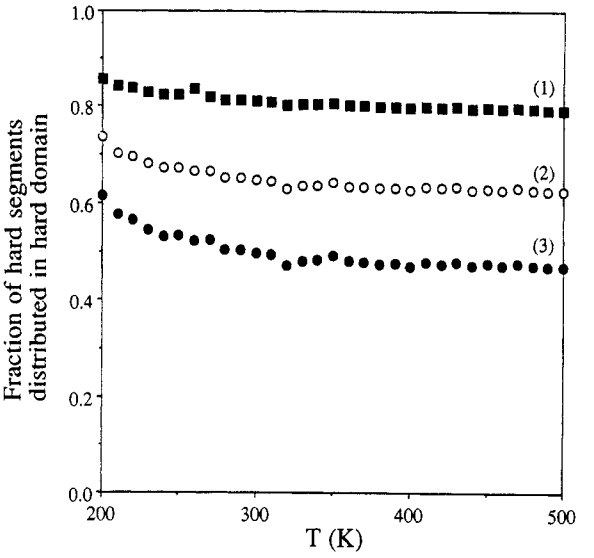

Figure 11. Effect of the soft-segment length on the fraction of hard segments distributed in the hard-segment-rich domain, F_{HH}: (1) M24M/PPG-1000; (2) M24M/PPG-2000; (3) M24M/PPG-3000. V is taken to be 15 kcal/mol in all cases.

on the T_g of the soft segments. Higher T_g values are usually correlated with lower degrees of phase separation.[36] It is, however, impossible to extract the exact phase composition from T_g changes as at least two factors contribute to changes in the T_g of polyurethane soft segments. First, the "copolymer" effect due to the hard segments dissolved in the soft phase is the only contribution taken into account to calculate the phase composition.[36] Second, the "cross-linking" effect associated with confinement of the soft-segment chain end by virtue of its connection to the phase-separated hard domains will also increase T_g.[41-43] This effect is difficult to address quantitatively, however. Earlier measurements have, in fact, shown that it can dominate.[41-43] In addition, our calculation for the diacetylene chain extender system involves a more rigid unit compared to butanediol chain extender. This factor could also influence the degree of phase separation.

The effects of changing the soft-segment molecular weight are not clear. Although some thermal experiments measuring changes in T_g have been carried out for soft segments of different lengths, individual phase compositions have not been defined. Our calculated degree of phase separation for different soft-segment lengths is summarized in Figure 11. We predict that samples containing longer soft segments have a lower degree of phase separation. Although the observed large decrease in T_g with increasing soft-segment length might lead to the conclusion that phase separation increases with increasing soft-segment length, such changes have been interpreted to arise from the cross-linking effect mentioned above.[41-43]

Infrared spectroscopy is an alternate tool for measurement of the degree of phase separation. It is well accepted that an amide I band with lower frequency corresponds to hydrogen-bonded hard segments and the higher frequency component is associated with free hard segments dispersed in the soft-segment-rich domains.[19] F_{HH}'s can be determined using the relative heights of these two bands. In this way we measure F_{HH}'s to be 42.6, 34.9, and 30.7% for M24M/PPG-1000, -2000, and -3000, respectively. These measurements are to be compared with the calculated values of 80, 62, and 50%. The decrease in the degree of phase separation associated with samples containing longer soft segments derives from the fact that while the phase composition of the isotropic phase is very close for all samples considered, the overall hard-segment concentrations, ϕ_{2T}'s, change a great deal. These values are 37, 23, and 17% for M24M/PPG-1000, -2000, and -3000, respectively. It should also be mentioned that our calculations consider only monodisperse hard-segment lengths. No data are available for analysis of the monodisperse case. In addition, we assume that the hard–hard segment interaction parameter, V, is independent of the soft-segment length.

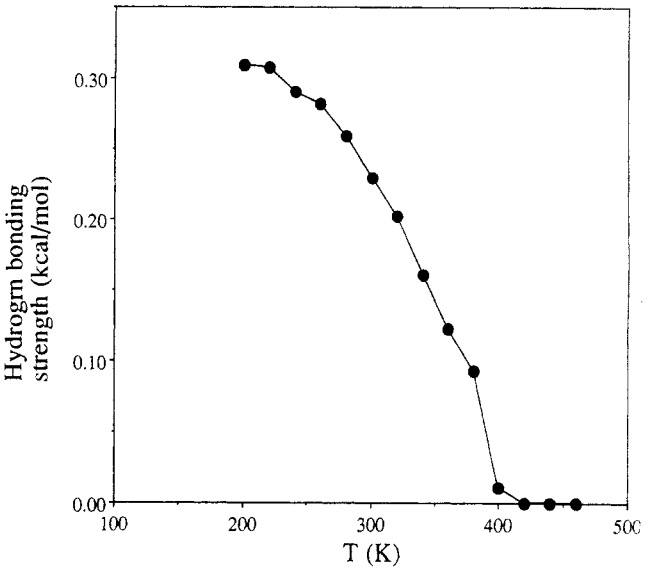

Figure 12. Simulated hydrogen-bonding strength at different temperatures for two isolated M24M hard segments described by the Maier–Saupe model.

Role of Various Secondary Forces. In our analysis, both the relative orientation of the hard segments and interchain interactions vary as a function of temperature. This is consistent with solid-state NMR data obtained for the MDI–BD copolymer which showed that the BD chain extender librates within an angular deviation of 12–16° in a temperature range from 62 to 83 °C.[44] At elevated temperatures, the degree of this librational motion for the hard segments increases, causing $\langle P_2 \rangle$ to decrease. This behavior is reflected by the apparent decrease of hydrogen bonds seen in infrared spectroscopy.[15] Variation in hydrogen bond strength with temperature for two M24M hard segments can be calculated utilizing simulation methods (eqs 14 and 16); results are presented in Figure 12. These results, consistent with experimental data,[15] are obtained for a simplified model since we assume that

the entire hard segment librates as a rigid rod without considering the local functional group dynamics and segmental migrations. A new interpretation of infrared data is thus provided. The generally accepted explanation for the decrease in the amount of hydrogen bonds observed in infrared with increasing temperatures is attributed either to thermal expansion effects or increased phase mixing. We propose that an increase of hard-segment libration can also possibly explain the reduction in the hydrogen-bonded component with negligible contributions from phase mixing. Hydrogen bonds are strong secondary forces but are of short range and highly directional. Steric interactions between phenyl rings generally inhibit hydrogen-bond formation. Our simulation studies demonstrate that departures from the ideal linear state, even at very small angles, will significantly diminish the strength of the hydrogen bond.

Chemical immiscibility of the hard-soft segments has long been suggested as the most important factor in the determination of polyurethane phase separation. More specifically, inter-urethane hydrogen bonds are regarded as stronger than hard-soft interactions, providing the driving force for phase separation. As mentioned in the Introduction, this hypothesis is inconsistent with spectroscopic data presented in the literature and illustrated as follows. The frequency of the infrared-active N–H stretching band reflects the relative strength of the various possible hydrogen bonds between the hydrogen and other functional groups. It has been proposed that stronger hydrogen bonds are directly associated with larger shifts in the N–H stretching frequency relative to the free N–H vibration.[8,9] In polyurethanes, the free N–H stretching vibration is usually observed at 3700 cm^{-1}. When hydrogen bonds to the ether oxygen, an N–H stretching vibration is observed at 3290 cm^{-1}. In contrast, the N–H stretching associated with the inter-urethane hydrogen bond is observed at 3350 cm^{-1}.[4,8] These results suggest that inter-urethane hydrogen bonds are not stronger than those between N–H and ether oxygen. Recently, *ab initio* calculations along with associated experimental studies have provided similar results.[9-11] In addition, other studies have concluded that the interaction parameter can be negative for phase-separated polyurethanes.[6,7] More studies are required to reach definitive conclusions about the relative strength of these hydrogen bonds.

Conclusions

This simulation study suggests that phase separation behavior in polyurethanes is due to the chain rigidity effect of the hard segments. Strong cohesive interactions between hard segments if packed in favorable orientations will make the hard segments separate into a hard-segment-rich phase coexisting with a soft-segment-rich phase. In many cases, with sufficiently long segment length, crystallization of hard segments further stabilizes the phase-separated structures. As expected, the hard-segment molecular weight greatly influences phase separation behavior. It is clear that samples containing longer hard segments exhibit a higher degree of phase separation. Although calculated values did not match experiments, the predicted trend was indeed verified. On the other hand, the effects of changing the soft-segment molecular weight are much more subtle. We predict that samples containing longer soft segments should contain a lower degree of phase separation, a suggestion consistent with infrared spectroscopic results. It is also our opinion that the thermal technique, particularly measurement of changes in T_g, cannot be used to measure the phase composition of polyurethanes.

By deconvoluting the overall calculated internal energy of the system, the contribution of hydrogen bonding to the interaction term has been calculated to be <17% with the remainder arising from van der Waals forces. Even though the strength of each hydrogen-bonding pair is stronger than van der Waals forces, the number of van der Waals interactions is much greater than the hydrogen-bonding contribution. Indeed, as mentioned before, studies have shown that polyurethanes without hydrogen bonds can also phase separate. Infrared spectroscopy is often cited to support the amount and extent of phase separation. For example, the relative intensity of hydrogen-bonded free carbonyl stretching versus the hydrogen-bonded component has been noted as primary evidence. On the basis of the present analysis, perhaps these spectroscopic analyses have provided only the characteristics of phase-separated structures and cannot explain the driving force for phase separation. This simulation study provides an opportunity for further studies in this area.

Acknowledgment. This research has been partially supported by a grant from the National Science Foundation, Polymers Program (DMR 8919105). We also acknowledge Molecular Simulations Inc. for the use of developmental software.

References and Notes

(1) Petrovic, Z. S.; Ferguson, J. *Prog. Polym. Sci.* **1991**, *16*, 695 and references therein.
(2) Hepburn, C. *Polyurethane Elastomers*; Applied Science Publishers: London, 1982.
(3) Culbertson, B. M., Ed. *Multiphase Macromolecular Systems*; Plenum Publishing Corp.: New York, 1989.
(4) Lee, H. S.; Hsu, S. L. *Macromolecules* **1989**, *22*, 1100.
(5) Chu, B.; Gao, T.; Li, Y.; Wang, J.; Desper, C. R.; Byrne, C. A. *Macromolecules* **1992**, *25*, 5724.
(6) Hwang, K. K. S.; Hemker, D. J.; Cooper, S. L. *Macromolecules* **1984**, *17*, 307.
(7) Hwang, K. K. S.; Lin, S. B.; Tsay, S. Y.; Cooper, S. L. *Polymer* **1984**, *25*, 947.
(8) Lee, H. S.; Wang, Y. K.; Hsu, S. L. *Macromolecules* **1987**, *20*, 2089.
(9) Bandekar, J.; Klima, S. *J. Mol. Struct.* **1991**, *263*, 45.
(10) Sun, H. *Macromolecules* **1993**, *26*, 5924.
(11) Bandekar, J.; Klima, S. *Spectrochim. Acta* **1992**, *48A*, 1363.
(12) Harrell, L. L., Jr. *Macromolecules* **1969**, *2*, 607.
(13) Kornfield, J. A.; Spiess, H. W.; Nefzger, H.; Eisenbach, C. D. *Macromolecules* **1991**, *24*, 4787.
(14) Christenson, C. P.; Harthcock, M. A.; Meadows, M. D.; Spell, H. L.; Howard, W. L.; Creswick, M. W.; Guerra, R. E.; Turner, R. B. *J. Polym. Sci., Polym. Phys. Ed.* **1986**, *24*, 1401.
(15) Rubner, M. F. *Macromolecules* **1986**, *19*, 2114.
(16) Blackwell, J.; Lee, C. D. *J. Polym. Sci., Polym. Phys. Ed.* **1983**, *21*, 2169.
(17) Paul, D. R., Newman, S., Eds. *Polymer Blends*; Academic Press: New York, 1978.
(18) Utracki, L. A. *Polymer Alloys and Blends*; Hanser Publishers: Munich, 1989.
(19) Coleman, M. M.; Graf, J. F.; Painter, P. C. *Specific Interactions and the Miscibility of Polymer Blends*; Technomic Publishing Co.: Lancaster, PA, 1991.
(20) Flory, P. J.; Abe, A. *Macromolecule* **1978**, *11*, 1119.
(21) Flory, P. J.; Ronca, G. *Mol. Cryst. Liq. Cryst.* **1979**, *54*, 311.
(22) Hølyst, R.; Schick, M. *J. Chem. Phys.* **1992**, *96*, 721; **1992**, *96*, 730.
(23) Liu, A. J.; Fredrickson, G. H. *Macromolecules* **1992**, *25*, 5551; **1993**, *26*, 2817.
(24) Fan, C. F.; Olafson, B. D.; Blanco, M.; Hsu, S. L. *Macromolecules* **1992**, *25*, 3667.
(25) Flory, P. J. *Adv. Polym. Sci.* **1984**, *59*, 1 and references therein.
(26) Stouch, T. R.; Jurs, P. C. *J. Chem. Inf. Comput. Sci.* **1986**, *26*, 4.
(27) Mayo, S. L.; Olafson, B. D.; Goddard, W. A., III *J. Phys. Chem.* **1990**, *94*, 8897.
(28) Lu, X.; Weiss, R. A. *Macromolecules* **1992**, *25*, 3242.
(29) Flory, P. J. *Proc. R. Soc. London* **1956**, *A234*, 73.
(30) Matheson, R. R., Jr.; Flory, P. J. *J. Chem. Phys.* **1980**, *73*, 6327.
(31) Flory, P. J. *Macromolecules* **1978**, *11*, 1138.

(32) Warner, M.; Flory, P. J. *J. Chem. Phys.* **1980**, *73*, 6327.
(33) Maier, W.; Saupe, A. *Z. Naturforsch.* **1959**, *14A*, 882; **1960**, *15A*, 287.
(34) Priestley, E. B.; Wojtowicz, P. J.; Sheng, P. *Introduction to Liquid Crystals*; Plenum Press: New York and London, 1975; Chapter 3.
(35) Koberstein, J. T.; Gàlambos, A. F.; Leung, L. M. *Macromolecules* **1992**, *25*, 6195.
(36) Koberstein, J. T.; Leung, L. M. *Macromolecules* **1992**, *25*, 6205.
(37) Dumais, J. J.; Jelinski, L. W.; Leung, L. M.; Gancarz, I.; Galambos, A.; Koberstein, J. T. *Macromolecules* **1985**, *18*, 116.
(38) Leung, L. M.; Koberstein, J. T. *Macromolecules* **1986**, *19*, 706.
(39) Hu, J.; Park, Y.; Painter, P. C.; Coleman, M. M. *Polym. Prepr. (Am. Chem. Soc., Div. Polym. Chem.)* **1982**, *29* (1), 321.
(40) Hu, X.; Stanford, J. L.; Day, R. J.; Young, R. J. *Macromolecules* **1992**, *25*, 672.
(41) Andrady, A. L.; Sefcik, M. D. *J. Polym. Sci., Polym. Phys. Ed.* **1983**, *21*, 2453.
(42) Feger, C.; MacKnight, W. J. *Macromolecules* **1985**, *18*, 280.
(43) Petrovic, Z. S.; Javni, I. *J. Polym. Sci., Polym. Phys. Ed.* **1989**, *27*, 545.
(44) Kintarnar, A.; Jelinski, L. W.; Gancarz, I.; Koberstein, J. T. *Macromolecules* **1986**, *19*, 1876.